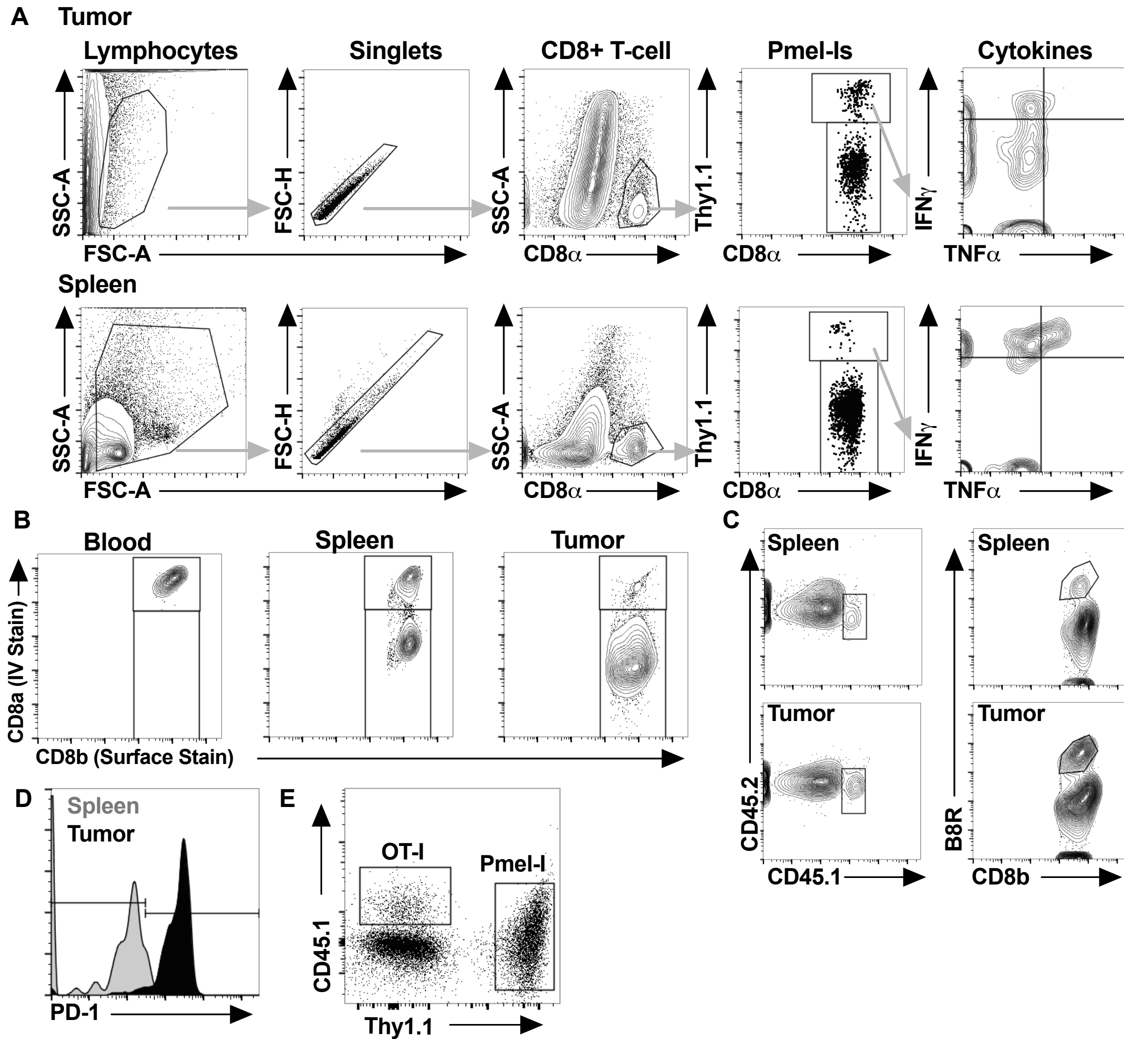

Supplemental figure 1: Representative gating strategies for CD8$^+$ T cells recovered from blood, tumors and spleens. A) Identification and functional analysis of Pmel-Is from spleens and tumors from Fig. 1 and 3 was accomplished as shown. B) Representative IV CD8α staining in the blood, spleen and tumor for Fig. 1, 2, 5, and 6. C) Representative identification of OT-Is and B8R-specific CD8$^+$ T cells for Fig. 5 and 6. D) Representative PD-1 gating of Pmel-Is in the spleen and tumor for Fig. 3, 4, 5, 6, 7. E) Representative gating for mixed OT-I (CD45.1$^+$) and Pmel-I (Thy1.1$^+$) in the tumor for Fig. 4.

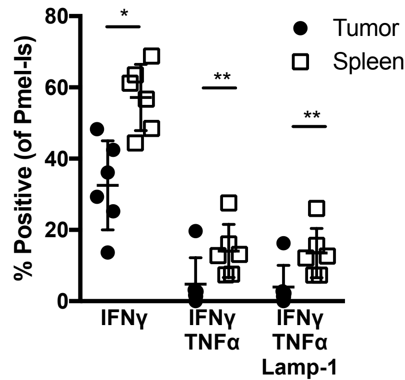

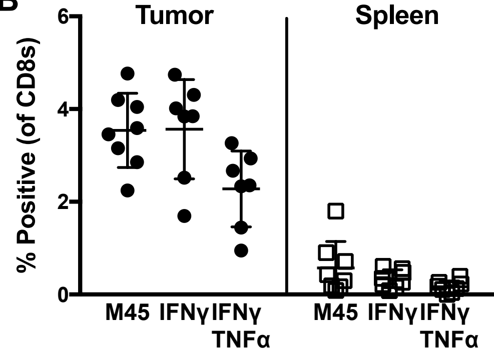

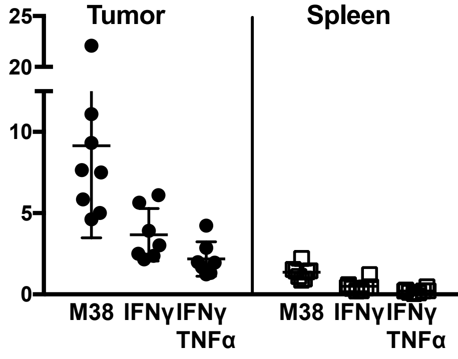

Supplemental figure 2: Function and PD-1 expression of TAA-specific and non-specific $CD8^+$ T cells in the tumor and blood. A) 10^4 Pmel-Is ($Thy1.1^+$) were transferred into naïve C57B6/J mice ($Thy1.2^+$) on D-1, given 1 x 10^5 B16F0s on D0, and infected with MCMV-gp100 on D5. Shown is the function (cytokine production and degranulation) of Pmel-Is in the tumor and spleen seven days post infection after *ex vivo* gp100 stimulation (n=6, 2 experiments). B) Cytokine-producing $CD8^+$ T cells were enumerated after *ex vivo* peptide stimulation (n=10) and compared to tetramer-binding cells in the tumor and spleen after MCMV-gp100 infection (mice from Fig. 1 and 3).

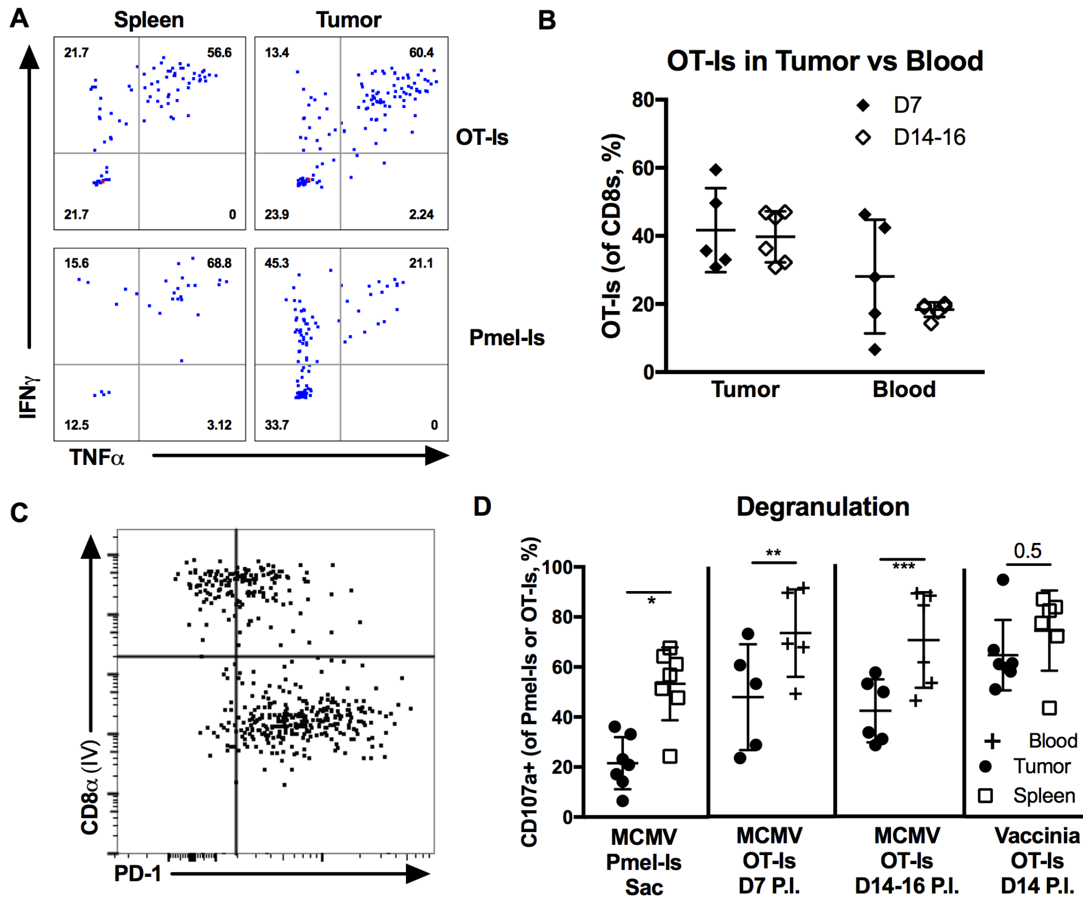

Supplemental Figure 3: Purified virus-specific CD8$^+$ TIL are more functional than purified TAA-specific CD8$^+$ TIL. A) To test the function of CD8$^+$ TIL after isolation from the tumor milieu, we used a co-adoptive transfer system that enabled analyses of both TAA-specific and virus-specific T cells from the same tumor simultaneously. We co-transferred OT-I (CD45.1$^+$) and Pmel-I (Thy1.1$^+$) TCR transgenic T cells into B6 mice (CD45.2$^+$, Thy1.2$^+$) on D-1, implanted B16F0 tumors on D0 and co-infected with MCMV-SL8 and MCMV-gp100 on D5 to drive the expansion of both OT-I and Pmel-I T cells. When tumors were >100 mm^2, CD8$^+$ TIL were enriched from the tumor homogenate with magnetic beads as described in the methods before stimulation with the SIINFEKL or gp100 peptide in the presence of M2-10B4 fibroblasts as APCs. Pmel-Is isolated from the tumor were more functional than Pmel-Is stimulated within the impure tumor homogenate (compare to Figure 3A). Nevertheless, these Pmel-Is remained markedly less functional than Pmel-Is recovered from the spleens of the same animals. In contrast, equivalent proportions of OT-Is isolated from the tumor and the spleen produced IFN-γ and TNF-α. B-C) Mice are from Fig. 3D-F. Shown is (C) the representative PD-1 expression of OT-Is that were labeled (tissue) or unlabeled (vasculature) by IV CD8α antibody, on D7 P.I. D) CD107a (Lamp-1,

degranulation) exposure after *ex vivo* peptide stimulation of tumor and virus-specific CD8s in the tumor, blood and spleen at different times post MCMV or VacV infections (same mice as Fig. 3 and 5).

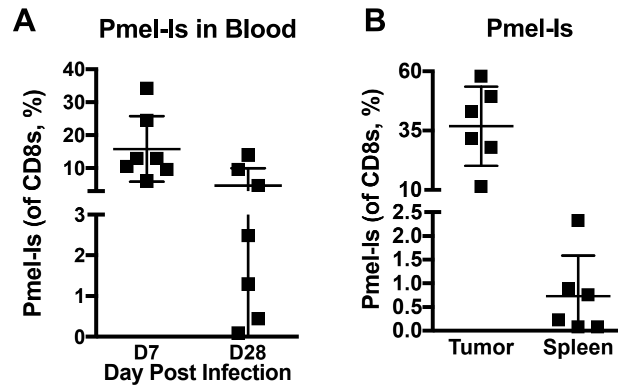

Supplemental figure 4: Pmel-Is in the blood, tumor and spleen at various time-points. From Fig. 6A and B. Shown is the frequency of Pmel-Is among $CD8^+$ T cells (A) in the blood before tumor implantation and (B) in the tumor and spleen 14-35 days after tumor implantation.